

**Copyright**

**By**

**Michael Andrew Wallen Jr.**

**2018**

The Thesis committee for Michael Andrew Wallen Jr

Certifies that this is the approved version of the following thesis:

Isolation and Characterization of *Pisum sativum* Apyrases,  
PsNTP9 and PsNTP9-DM, Cloned and Expressed in *Escherichia*  
*coli*

Approved by  
Supervisory Committee:

Supervisor: Stanley J. Roux

Enamul Huq

Isolation and Characterization of *Pisum sativum* Apyrases,  
PsNTP9 and PsNTP9-DM, Cloned and Expressed in *Escherichia*  
*coli*

Michael Andrew Wallen Jr.

Thesis

Presented to the Faculty of the Graduate School

of The University of Texas at Austin

in Partial Fulfillment of the Requirements

for the Degree of

Master of Arts

The University of Texas at Austin

May 2018

## Acknowledgements

I would like to thank Dr. Stan Roux, Dr. Greg Clark, and Dr. Han-Wei Jiang for allowing me to learn under their guidance, and for trusting me. I am deeply grateful for the pleasure of being able to work in the lab with each of you, and the wonderful staff and students I've seen making progress each day. I always knew I could count on someone to be available to answer a hard question or give some good advice.

I would also like to thank Dr. Mona Mehdy, who sponsored me early and helped me to learn how to work in a molecular biology lab, and encouraged me to be confident and self-sufficient. I also have an enormous amount of gratitude for the CNS graduate staff, whose efforts made my attendance possible, and who could be counted upon to help me out whenever I needed it.

I owe thanks to my cohort and others in the Plant Biology Department for fostering our community and making me feel cared for and welcome. Samsad Razzaque, Ash Nelson, Chaehee Lee, Bikash Shresthra, Nathan LeClear, and a multitude of others.

My wife Cathy supported me every day. She inspired me to work hard by finishing her MBA, and working to protect and service the community with Teacher Retirement Services. She supported me with words of encouragement, nourishment when I had tunnel vision, and most importantly love.

Michael Andrew Wallen Jr, M.A.

The University of Texas at Austin, 2018

Supervisor: Stanley J Roux

Adenosine triphosphate (ATP) is widely known as a fuel source for many biochemical processes, and to a lesser degree also as a signaling molecule in plants and animals. When plants are subjected to biotic or abiotic stress or undergoing exocytosis, they release ATP into the extracellular matrix (ECM). The release of ATP sets off a signal transduction pathway, first rapidly increasing the concentrations of cytosolic calcium, reactive oxygen species, and nitric oxide. How these changes specifically influence physiology is the object of much research in both plants and animals. Some of the changes that are affected influence growth and development, stomatal function, and gravitropism. Apyrases and other phosphatases control the concentration of the released nucleotides by breaking phosphate bonds from nucleoside triphosphates and diphosphates. Research aimed at the discovery of receptors, signaling pathway components, and processes has been successful to some extent. There are now known purinergic receptors in both plants and animal cells.

We have cloned a truncated version of *Pisum sativum* (ps) NTP9. We used a pET-22B vector to add a histidine tag and transformed the vector into the BL21 *Escherichia coli* with a T7 promoter to enable IPTG induction of the LAC operon and expression of the enzyme. The pET-22B vector was incubated in separate samples with BL21 cells. Cells were propagated, and the expression of recombinant proteins

PsNTP9, and separately, a double mutant PsNTP9-DM with a second calmodulin-binding domain, were induced ectopically. Cells were broken open by shaking them and mixing them with lysis buffer. Centrifugation was performed to separate the supernatant containing the released apyrases from the particulate wall fraction. The enzymes were purified by affinity chromatography, then their purity was evaluated by sodium dodecyl sulfate - polyacrylamide gel electrophoresis (SDS-PAGE). Western blots were performed to verify presence of the apyrases using a commercial anti-histidine antibody to detect PsNTP9 and PsNTP9-DM. Once suitable amounts of our proteins of interest were harvested, we performed Bradford assays to determine the protein concentration of the samples and carried out an apyrase activity assay to determine the specific activity of the purified enzymes and compare it to that of other known apyrases.

# Table of Contents

Chapter 1: Introduction .....	1
Chapter 2: Cloning and transformation of <i>Escherichia coli</i> with plasmid vector.....	5
2.1 Materials and Methods	
2.1.1 The bacterial vector.....	5
2.1.2 Transformation of BL21(DE3) cells .....	5
2.2 Results .....	6
Chapter 3: Growth of transformed BL21 cells, expression, fractionation, purification and detection of PsNTP9 and PsNTP9-DM.....	7
3.1 Materials and Methods	
3.1.1 Growth and expression.....	7
3.1.2 Fractionation of cells.....	8
3.1.3 Purification with IMAC resin .....	8
3.1.4 Detection and identification of purified PsNTP9 and PsNTP9-DM.....	9
3.2 Results .....	10

Chapter 4: Apyrase activity assay and phosphate assay	
4.1: Materials and methods	
4.1.1 Apyrase activity assay.....	12
4.1.2 Phosphate assay .....	13
4.2 Results .....	14
Chapter 5: Figures.....	15
Chapter 6: Discussion.....	26
Chapter 7: Conclusions.....	31
References.....	33
Vita .....	37



## List of Figures

Figure 2.1.1 The pEt22B vector.....	20
Figure 2.1.2A PsNTP9 Full length CDS.....	21
Figure 2.1.2B Truncated PsNTP9 CDS .....	22
Figure 2.1.2C PsNTP9-DM Full length CDS.....	23
Figure 2.1.2D Truncated PsNTP9-DM CDS and Figure 2.1.2 caption.....	24
Figure 2.1.3A PCR product of PsNTP9–pET22B.....	25
Figure 2.1.3B. PCR product of PsNTP-9-DM.....	25
Figure 2.1.3C Colony PCR of PsNTP9-pET22B.....	25
Figure 2.1.3D Colony PCR of PsNTP9-DM – pET22B and Figure 2.1.3 caption.....	26
Figure 2.1.4 PsNTP9-DM mutations and primers for cloning and colony PCR.....	26
Figure 2.2 Immunoblot analysis of purified psPsNTP9 and PsNTP9-DM .....	28
Figure 3.1.1 Truncated PsNTP9-DM purification on affinity column after periplasmic expression in E. coli .....	29
Figure 3.2.1 Immunoblot analysis of purified PsNTP9 and PsNTP9-DM after elution from affinity column.....	30
Figure 3.2.2 Coomassie-blue stained SDS-PAGE of purified PsNTP9 and Ps-NTP9-DM.....	31

## Chapter 1 – Introduction

In order to survive, plants must react to their environments chemically. This is true at both the organismal level and the cellular level. Some responses need to be relatively quick, like a response to herbivory or infection. An initial signal is perceived in response to an external or internal stimulus, which initiates a signal transduction chain reaction that causes a cellular response, such as a change in gene expression. In response to many biotic and abiotic stimuli, signaling molecules are released from cell membranes to signal the appropriate response at the correct location. Certain chemicals are used for extracellular communication of transducing signals, such as hormones, or neurotransmitters in animals. For each type of signaling molecule, there is a corresponding type of receptor. Intercellular signals must be transduced across the cell membrane to take effect in a cell.

Extracellular ATP (eATP), and other nucleotides are known to be an intercellular signaling molecule in both plants and animals. The receptors that respond to these signals are termed purinergic (Burnstock, 1972). Many different physiological responses to eATP have been identified in plants, animals, and microbes. Though the details of signal transduction may not yet be known, multiple purinergic receptors (purinoceptors) have been identified in animals, however, until 2014 there was no published research that identified a plant eATP receptor with an extracellular domain. This purinergic receptor, called DORN1, was identified in *Arabidopsis*, (Choi et al., 2014). This contributed validity to the study of eATP as an intercellular signaling molecule in plants. Without an eATP receptor in the ECM, it was unclear how an eATP signal could be transduced into a physiological response.

Purinergic receptors have been divided into 2 classes called P1 and P2. Only adenosine and AMP can be bound by P1 receptors, but the P2 receptors bind ADP, ATP, and many other nucleoside di- and triphosphates. P2 purinoceptors are further divided into type P2X, the ligand-gated subtype, and P2Y, the G-protein-coupled subtype. When P2 receptors are activated in animal cells, the cytosolic calcium concentration increases rapidly. This also happens in plant cells (Burnstock, 2007) (Jeter et al., 2004) (Demidchek, 2009). Plant purinoceptors can also be blocked by the same antagonists as animal purinoceptors (Song et al. 2006). Despite these shared characteristics, there is very little structural similarity between plant and animal purinoceptors. The study of animal P2X receptors, and a search for sequence similarity did lead to the discovery of a purinoceptor with strong sequence similarity in *Ostreococcus tauri*, a unicellular green alga (Fountain et al., 2008).

DORN1 was discovered through the study of a plasma-membrane-bound lectin receptor-kinase with high affinity for ATP (LecRK1-9). Knocking-out LecRK1-9 in *Arabidopsis*, resulted in a null mutant unable to increase its cytosolic calcium concentration in response to treatments. With this finding, the original protein was renamed to Does Not Respond to Nucleotides 1 (DORN1) in reference to the null mutant, and the knockout that facilitated its discovery.

There are 45 lectin-receptor kinases (LecRK) in *Arabidopsis*, many of which have large extracellular domains (Clark et al., 2014). Though some have already been ascribed other unrelated functions, many are considered as candidates for additional purinoceptors. Patch-clamp studies of the kinetics of cellular uptake of calcium revealed a dynamic range (Demidcheck, 2011), which lends support to the idea of

there being two types of P2 purinoceptors in plants, as there are in animals (Roux, 2014).

The advantage of being able to respond quickly to increased concentrations of eATP is likely that it grants the ability to induce defense responses in a timely manner (Clark and Roux, 2011). Following the increase in cytosolic calcium concentration, there is a rapid increase in reactive oxygen species (ROS), including superoxides and peroxides, and nitric oxide (NO) (Tanaka et al., 2010). Additionally, the NADPH oxidase enzyme that catalyzes superoxide production is stimulated by increased cytosolic calcium (Monshausen, 2009). Increased levels of ROS and NO are linked to increased expression of mitogen-activated protein kinase (MAPK) genes, which are regular members of signal transduction cascades from cytoplasm to nucleus (Jeter et al., 2004; Song et al., 2006; Choi et al., 2014).

Alternatively, it has been proposed that eATP induces plant defense responses mediated through activation of intracellular signaling by jasmonic acid (JA) (Tripathi et al., 2018). They asserted that other JA signaling components are affected by increased eATP, and further suggested direct cross talk between eATP and JA in intracellular signaling events.

The release of eATP at wound sites causes a responding increase in the expression of apyrase genes (Lim et al., 2014). These enzymes then act to lower the amount of eATP and dampen the effects by hydrolyzing phosphates from ATP and ADP (Song et al., 2006). Fluctuations in extracellular nucleotide concentrations affect growth (Roux et al., 2007), and stomatal function (Clark et al., 2011; Hao et al., 2012). As cells expand during normal growth, they release eATP that can stimulate or stunt growth, depending upon the induction of ROS and NO signals in a dose-dependent

manner (Clark and Roux, 2011). It is expected that influence on auxin transport is the mechanism by which eATP affects growth (Tang et al., 2003; Liu et al., 2012).

As in all higher life forms, the biochemical systems within plants are highly integrated. The use of feedback loops in signaling are necessary to help prevent one system from overrunning another in a way that negatively affects the survival of the organism. In short, all signals need to be turned off once they've run their course. Extracellular apyrases as well as extracellular phosphatases are the regulators of extracellular nucleotide signals, and they stop purinoceptors from being activated by hydrolyzing their agonists.

## Chapter 2: Cloning and transformation of BL21 *Escheria coli* with plasmid vector

### 2.1 Materials and methods

#### 2.1.1 The bacterial vector

The plasmid was provided to Roux Lab by the Maynard Lab, in the Department of Chemical Engineering (CPE 5.456). The vector was crafted using the pET-22b(+) plasmid, and includes an N-terminal signal sequence for periplasmic localization attached to a truncated PsNTP9 with a C-terminal His•Tag® sequence. The plasmid also contains a hybrid T7 LAC promoter and the *lacI* gene encoding the Lac repressor, which makes transcription under the T7 promoter inducible by the addition of IPTG to the bacterial culture, and also carries ampicillin resistance. The PsNTP9 and PsNTP9-DM apyrase protein constructs are N-truncated, in order to use the periplasmic localization signal of the pET-22b plasmid, shown in figure 2.1.1

#### 2.1.2 Transformation of BL21(DE3) cells

The plasmids featuring PsNTP9 and PsNTP9-DM constructs were incubated overnight with DH5α *E. coli* and plated on LB agar with ampicillin. After growth the colonies were PCR cycled. The PsNTP9 and PsNTP9-DM genes, and cloning and PCR primer sequences are shown in figure 2.1.2 A-D, and figure 2.1.3. The DH5α strain was used to transform BL21-DE3 *E. coli*, which were used for expression. Then transformation was verified by sequencing, at the MBS core facility.

## 2.2 Results

The pET22B vector was an excellent tool. Competent cells were transformed successfully, and were segregated using the plasmid's antibiotic resistance. Transformation was verified by sequencing the incorporated plasmid in the MBS core facility. PCR products and colony PCR results are shown in figure 2.2.1. The designed genetic mechanisms of periplasmic location, and induction using IPTG and the Lac operon, allowed control of expression and localization of PsNPSNTP9 and PsNTP9-DM to the periplasm. Upon testing IPTG induction, the expressed histidine tags on PsNTP9 and PsNTP9-DM were detected by immunoblot (Figure 2.2).

## Chapter 3: Growth of transformed BL21 cells, expression, fractionation, purification and detection of PsNTP9 and PsNTP9-DM

### 3.1 Materials and methods

#### 3.1.1 Growth and expression

The following steps were completed for PsNTP9 and PsNTP9-DM samples: transformed BL21 cells were inoculated to a 2 mL Terrific Broth (TB) with ampicillin and 1% glucose media, and shaken for 5 hours in two sets of PsNTP9 and PsNTP9-DM transformed cells, at 30°C and 37°C variables, for a total of 4 samples. The 2 mL starters were then used to inoculate 4 separate 500mL volumes which were incubated overnight at 37C at 225 rpm on a shaker table. The following day the cultures were harvested and transferred into 250 mL centrifuge bottles. These were centrifuged for 10 minutes at 5K rpm in a Beckman with JA-10 rotor. Then each sample was decanted and the pellet was resuspended in 20 mL of media with antibiotic, and then returned to a fresh batch of 500ml of media with antibiotic.

Next, expression was induced by addition of 500  $\mu$ L of 1M IPTG to each sample, and they were shaken at 25°C for 5 hours. Then cultures were harvested and centrifuged 10 minutes and decanted. Pellets were saved overnight in a -80°F freezer.

Later repetitions of this procedure involved optimization and the 37°C incubation temperature variable was no longer used after the initial experiment. Western blot figure 3.1.1 shows greatest induction at 30°C.



### 3.1.2 Fractionation of cells

Frozen pellets were thawed and resuspended in 20 mL of cold sucrose solution (0.75M sucrose, 0.1M Tris adjusted to pH 8.0 with HCL, filtered, 4°C), and transferred equally to 45 mL Falcon tubes. 1 mL of 10 mg/mL lysozyme in sucrose solution was added to each tube, and 10 mL of 1mM EDTA was added drop-wise with gentle shaking. The samples were then shaken at 4°C for 1 hour, and 0.5 mL of MgCl<sub>2</sub> was added drop-wise while shaking. The samples were shaken again at 4°C for 1 hour and centrifuged 20 minutes at 20K rpm. Supernatant was then transferred to Snakeskin dialysis tubing and dialyzed against 4L of dialysis buffer (10mM Tris pH 8.0, 0.5M NaCl). This was done in order to remove EDTA to prevent interference with the IMAC recovery step.

Optimization dictated that later fractionations use 15 mL of cold sucrose, rather than 20 mL. This was changed to effectively increase the concentrations of the other reagents in the procedure, in order to increase the effectiveness of apyrase protein extraction. On April 13, a second fractionation protocol was substituted, though the results were unfavorable, so it was only used that once, and the original protocol was used for later repetitions.

### 3.1.3 Purification with IMAC resin

In separate tubes 1 mL IMAC resin was washed in each of 4 Biorad disposable columns with 10 mL water, followed by 2mL Ni<sup>2+</sup> charging buffer (50mM nickel sulfate), then 10 mL of wash buffer (20mM Tris pH 8.0, 0.5M NaCl, 20mM imidazole). Each dialysate was transferred to a 45 mL Falcon tube, and adjusted to 10mM imidazole from 1M stock. Next the prepared resin was divided, 0.5 mL each into the

Falcon tubes with dialysate, and the samples were shaken at 4°C for 4 hrs. Then the samples were centrifuged at 1K for 2 minutes and decanted to collect the resin, which was resuspended in 10 mL of wash buffer and centrifuged again and decanted. The samples were resuspended once more and the resin was collected by pouring into the columns. Then the columns were washed once more with 10 mL of wash buffer. Initially, the columns were eluted with 1mL of elution buffer, but on March 19<sup>th</sup> the elution volume was increased to 4 mL. During elution the color of the resin was observed to turn white, which indicates successful elution.

Starting on March 13, we began charging the IMAC resin with 10 mL of 0.2M Ni<sup>2+</sup> charging buffer. This was done in order to potentially increase the binding strength and volume of nickel held in the resin, so that more protein could be bound and eluted. Protein concentrations were determined using the Bradford method.

#### 3.1.4 Detection and identification of purified PsNTP9 and PsNTP9-DM

Samples were heated to 96°C for 10 minutes, then run on SDS- PAGE, 4-12% polyacrylamide 1.5 mm gel in MOPs running buffer at 150V. Gels were stained with Coomassie blue on a shaker table at room temperature (RT) for 2 hrs. Poured off Coomassie Blue stain, and added destaining buffer. Destaining buffer was changed after 20 minutes, then again after 1 hour, and allowed to sit on the shaker table overnight at RT. Eluate showed single visible bands for each of the purified samples at ~47 KD. This indicated that the proteins of interest were present and Western blots (WB) were performed for confirmation. Blotted to PVDF membrane, blocked the background with 5% milk with PBST, and treated with a commercial horse radish

peroxidase (HRP) conjugated antibody called HisProbe™ (Thermo-Scientific #15165)1:3500, prepared in 5% milk, to identify the presence of the histidine tags of our constructs. The blot was then treated with ECL substrate and visualized in the G:box imager in the MBS core facility.

In order to increase the effectiveness of the blot transfer, starting on March 21st, the PVDF membrane was soaked in methanol, 12 filters were used, and they were presoaked in 1M Tris-Gly and 40% methanol and 1%SDS.

### 3.2 Results

Cell propagation was without issues, cells were able to colonize new ampicillin containing media in high concentration. Immunoblots performed on extract of induced cells showed good signal. The fractionation procedure was verified to work well, given the concentration of protein samples run on SDS PAGE and Western blot. Some optimization was attempted, though even against Qiagen's "Protocol for preparation of 6XHis-tagged periplasmic proteins from *E.coli*," the initial fractionation procedure outperformed, providing higher concentrations of purified protein. Western blot of purified PsNTP9 showing concentrations after induction and purification is figure 3.2.1.

The purification procedure seemed to work well during execution, the IMAC resin turned blue when charged, and turned back white during elution, indicating that the resin bound the nickel in the charging buffer, and released it during elution. However, as the yield was less than expected, the concentration of the charging buffer was amplified by 80x. Similarly, 10 mL of 0.2M of charging buffer was used to

potentially increase binding and thus yield. The results from this are in figure 3.2.2. Doubling the imidazole concentration of the elution buffer was attempted next. Though it was possible to elute workable volumes from the affinity column, it is expected that much of the PsNTP9 and PsNTP9-DM proteins remained bound to the resin. This could be due to aggregation with other proteins with multiple histidine residues, or due to the high specificity of the columns for our proteins of interest (6 contiguous histidines). It could also be due to overexpression of our proteins of interest during the induction phase causing aggregation, and formation of inclusion bodies which can complicate binding and elution. Incubation time with the resin was increased from 4 to 5 hours. Since dialysis was also performed before detection, it was not ruled out as a suspect for loss of protein, so a protease inhibitor cocktail was added to the dialysis tubes. Though the combined effect of these changes allowed for elution of detectable quantities of purified protein, it is expected that some of the extracted protein was being kept bound to the resin. SDS PAGE gels and Western blots often showed a lower than desired signal, though some blots were successful, and bound antibodies with a strong signal. (Fig. 3.2.1)

## Chapter 4: Apyrase activity assay and phosphate assay

### 4.1: Materials and methods

#### 4.1.1 Apyrase activity assay

We followed the protocol described by Steinebrunner et al. (2000), *Molecular and biochemical comparison of two different apyrases from Arabidopsis thaliana*, for the apyrase activity assay.

Prior to performing this step, the purified PsNTP9 and PsNTP9-DM apyrase samples selected for potentially higher protein concentrations were dialyzed to remove the elution buffer. The assay was performed in duplicate on a 96 well plate. Selected PsNTP9 and PsNTP9-DM samples were incubated in assay buffer (100  $\mu$ L 60mM HEPES pH7.0, 3mM MgCl<sub>2</sub>, 3mM CaCl<sub>2</sub>) prepared separately with 3mM ATP, and AMP substrates at 4 different volumes of substrate per preparation (50,100,150, and 200  $\mu$ L). This was done for optimization, and we noted that 50  $\mu$ L of substrate with 100  $\mu$ L buffer was sufficient from results. The ATP and AMP substrate stocks were 100mM prepared in 2 mL HEPES buffer. The substrate stocks were aliquoted into 2mL Eppendorf tubes. All variable reactions were carried out as follows: 100  $\mu$ L of apyrase assay buffer, including substrate, was added to each of the variable plate wells and negative control (buffer only in 1 well). The positive control used IPTG induced raw cell lysate and stock concentration ATP. Then 50-200  $\mu$ L of the purified and dialyzed PsNTP9 and PsNTP9-DM samples were added to their designated wells. Then the plate was covered in foil and placed on a shaker platform for 1 hour 45 minutes at RT, after which it was taken to the MBS core facility to have the plate read in a spectrophotometer.

This assay was repeated, adding the substrate ADP prepared as described above, and using the same controls. Each of the 4 apyrase samples (PsNTP9 and PsNTP9-DM purified on 3/28, and PsNTP9 and PsNTP9-DM purified on 4/19) was represented using 8 wells for each substrate (2 wells each for PsNTP9 and PsNTP9-DM purified on each date). This time the protein samples were all in 50  $\mu$ L volumes. After filling the wells, the plate was wrapped in foil and placed on a shaker platform for 1 hour 30 minutes.

#### 4.1.2 Phosphate assay

This colorimetric assay was originally performed on the same microtiter plate as the apyrase activity assay. First a standard curve was created using known molarities of ATP ranging up to 200 $\mu$ M. The first phosphate assay was done with corresponding volumes to the first apyrase assay run, except at  $\frac{1}{2}$  total volume to allow for addition of the reagent C without overfilling. The wells were first loaded with 125  $\mu$ L of reagent C. Reagent C components were prepared ahead and mixed the day of the assay. The recipe includes 2 mL water, 1 mL 6N sulfuric acid, 1 mL of 2.5% ammonium molybdate and 1 mL 10% ascorbic acid.

Once the wells were loaded with 125  $\mu$ L of reagent C, the reactions for each condition of the apyrase assay were transferred to 2 wells each, with 8 wells used per completed reaction. The positive control was one well for ATP alone, and the negative control was one well with reagent C alone. The phosphate assay reactions were allowed to incubate for 1 hour 10 minutes at 25°C. Then the plate was taken to the MBS core facility and read. The next phosphate assay was performed using a separate plate, and 3 substrates were used: ATP, ADP, and AMP, and each

phosphate assay reaction was done in triplicate, except for AMP, which was only done in duplicate since little to no activity was expected. Results are shown in figure 4.1.2.

#### 4.2 Results

There were no problems in executing the procedures other than a few errors in pipetting, which were corrected. The visual indication of activity was given with the colorimetric phosphate assay. First a standard curve was created using known concentrations of phosphates, and the results were linear as expected. The validity of the standard curve, apyrase activity and phosphate assays were confirmed when the plates were read. The color change (clear to light blue to dark blue) began very quickly for PsNTP9, especially with ATP. PsNTP9-DM samples changed more slowly and when the assay was ended after 1 and half hours, the color of the PsNTP9+ATP wells were the darkest, followed by PsNTP9-DM+ATP, which was close in color to PsNTP9+ADP and PsNTP9-DM+ADP. All wells with AMP stayed a very light blue. The results are shown in figure 4.2.

## Chapter 5: Figures

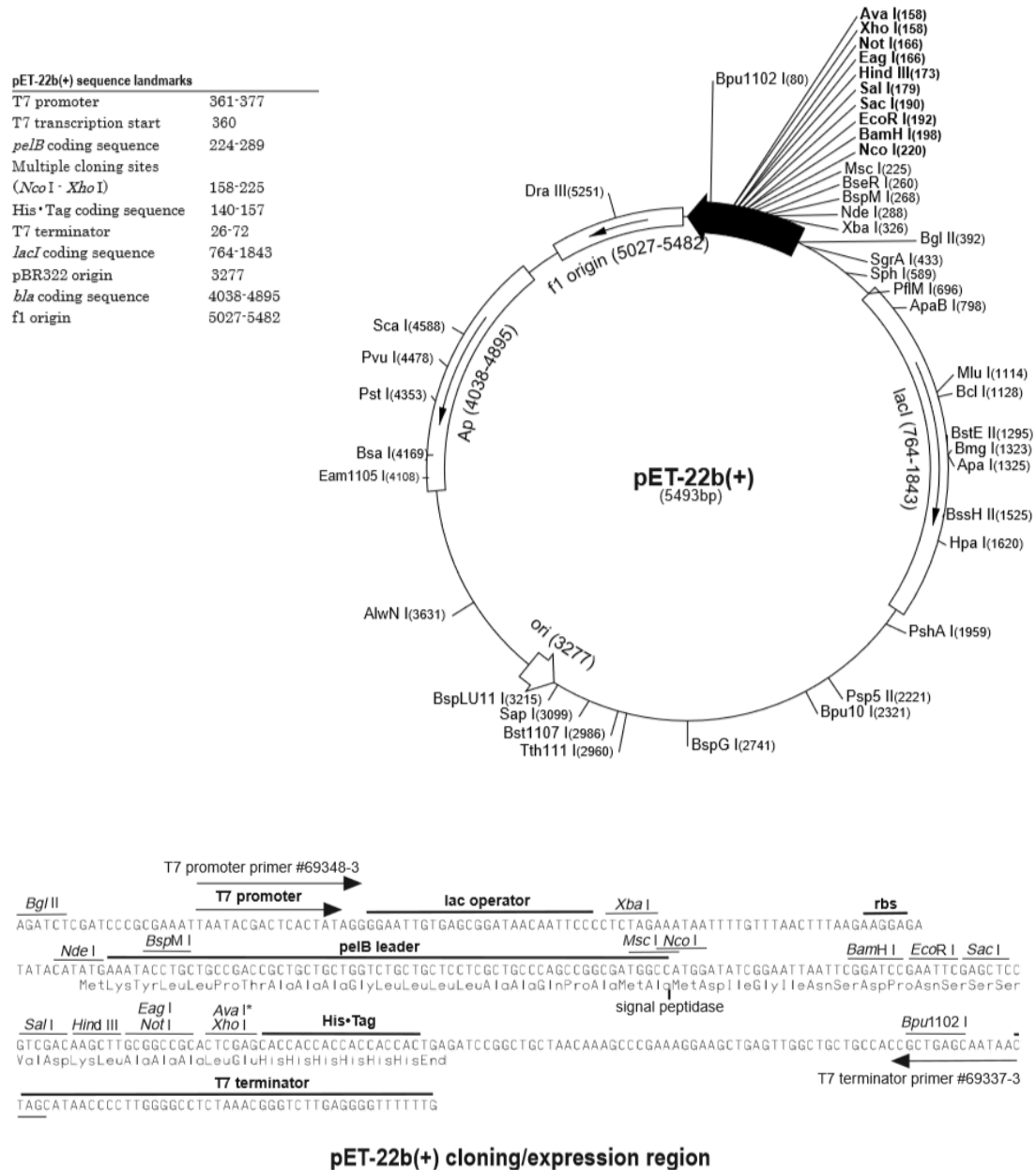


**Figure 2.1.1** : The pET-22b(+) vector carries an N-terminal *pelB* signal sequence for potential periplasmic localization, plus optional C-terminal His•Tag® sequence. Unique sites are shown on the circle map. Note that the sequence is numbered by the pBR322 convention, so the T7 expression region is reversed on the circular map. The cloning/expression region of the coding strand transcribed by T7 RNA polymerase is shown below (at bottom). For PsNTP9 and PsNTP9-DM insertion the sites where the plasmid was cut are between *Nco*I and *Bam*H I.



## 2.12 A

### PsNTP9-Full length CDS

ATGGAGCTCCTTATTAACTTATCACTTTTCTACTATTTTCTATGCCTGCAATCAC  
CTCCTCCCAATACTTAGGAAACAACCTACTCACCAGTAGAAAGATTTTCCTAAAAC  
AAGAGGAAATTTCTCTTACGCTGTAGTATTCGATGCTGGTAGCACCGGTAGTCGC  
ATTCATGTTTACCATTTTAACCAGAACCTAGATCTTCTTCATATTGGCAAAGGTGT  
TGAGTATTATAATAAGATAACACCTGGTTTGAGTTCATACGCTAATAATCCAGAAC  
AGGCTGCAAAATCTCTCATTCCACTTTTAGAGCAAGCAGA  
AGATGTCGTCCCCGACGATCTTCAACCCAAGACACCCGTTAGACTTGGGGCAACTG  
CCGGTTTAAGGCTTTTGAATGGAGATGCTTCTGAAAAGATATTGCAATCGGTAAGG  
GATATGCTGAGCAACAGAAGTACCTTCAACGTTCAACCAGACGCAGTTTCTATAAT  
TGATGGAACCCAAGAAGGTTCTTATCTATGGGTGACAGTTAACTATGCATTGGGAA  
ATTTAGGGAAAAAGTACACAAAAACAGTTGGAGTAATAGATCTTGGAGGTGGATCA  
GTTCAAATGGCGTATGCAGTATCAAAGAAAACCTGCTAAA  
ATGCTCCAAAAGTTGCAGATGGAGATGATCCATACATCAAGAAGGTTGTAICTCAAG  
GGAATACCATATGATCTCTATGTTACAGTTACTTACACTTCGGTAGAGAAGCATC  
TCGAGCAGAGATTTTGAAGCTCACTCCTCGTTCTCCTAACCCCTTGCCTTTTAGCTG  
GATTTAATGGAATCTATACATATTCAGGAGAAGAGTTTAAGGCAACTGCTTACACT  
TCTGGTGCAAACCTTTAATAAATGCAAAAACACAATTCGTAAGGCTCTTAAGTTGAA  
CTATCCTTGTCATATCAGAATTGCACCTTTTGGTGGAATT  
TGGAATGGTGGAGGAGGAAATGGACAGAAAAACCTTTTGGCTTCTTCATCTTTCTT  
TTACCTACCTGAAGATACCGGTATGGTTGATGCAAGCACACCTAATTTCACTTTC  
GGCCGGTCGATATTGAGACTAAAGCTAAAGAAGCTTGC GCGTTAAACTTCGAGGAT  
GCGAAATCTACTTATCCATTTCTTGATAAGAAAAATGTAGCTTCATATGTATGCAT  
GGATCTTATATATCAGTATGTGTTACTCGTTGATGGATTTGGTCTTGATCCATTGC  
AAAAGATTACATCAGGGAAGGAAATTGAATACCAAGATGC  
TATTGTGGAAGCTGCATGGCCTCTAGGCAATGCTGTAGAAGCCATATCAGCTTTAC  
CTAAATTTGAGCGATTGATGTATTTTGTTTAA

## 2.12 B

### Truncated-PsNTP9 CDS

GAAATTCCTCTTACGCTGTAGTATTCGATGCTGGTAGCACCGGTAGTCGCATTCA  
TGTTTACCATTTTAAACCAGAACCTAGATCTTCTTCATATTGGCAAAGGTGTTGAGT  
ATTATAATAAGATAACACCTGGTTTGAGTTCATACGCTAATAATCCAGAACAGGCT  
GCAAAATCTCTCATTCCACTTTTAGAGCAAGCAGAAGATGTCGTCCCCGACGATCT  
TCAACCCAAGACACCCGTTAGACTTGGGGCAACTGCCGGTTTAAGGCTTTTGAATG  
GAGATGCTTCTGAAAAGATATTGCAATCGGTAAGGGATAT  
GCTGAGCAACAGAAGTACCTTCAACGTTCAACCAGACGCAGTTTCTATAATTGATG  
GAACCCAAGAAGGTTCTTATCTATGGGTGACAGTTAACTATGCATTGGGAAATTTA  
GGGAAAAAGTACACAAAACAGTTGGAGTAATAGATCTTGGAGGTGGATCAGTTCA  
AATGGCGTATGCAGTATCAAAGAAAAGTCTAAAAATGCTCCAAAAGTTGCAGATG  
GAGATGATCCATACATCAAGAAGGTTGTAAGGGAATACCATATGATCTCTAT  
GTTACAGTTACTTACACTTCGGTAGAGAAGCATCTCGAG  
CAGAGATTTTGAAGCTCACTCCTCGTTCTCCTAACCCCTTGCCTTTTGTAGCTGGATTT  
AATGGAATCTATACATATTCAGGAGAAGAGTTTAAAGGCAACTGCTTACACTTCTGG  
TGCAAACCTTTAATAAATGCAAAAACACAATTCGTAAGGCTCTTAAGTTGAACTATC  
CTTGTCATATCAGAATTGCACTTTTGGTGGAAATTTGGAATGGTGGAGGAGGAAAT  
GGACAGAAAACCTTTTGTCTTCTTCATCTTTCTTTTACCTACCTGAAGATACCGG  
TATGGTTGATGCAAGCACACCTAATTTCATACTTCGGCCG  
GTCGATATTGAGACTAAAGCTAAAGAAGCTTGCGCGTTAAACTTCGAGGATGCGAA  
ATCTACTTATCCATTTCTTGATAAGAAAAATGTAGCTTCATATGTATGCATGGATC  
TTATATATCAGTATGTGTTACTCGTTGATGGATTTGGTCTTGATCCATTGCAAAAG  
ATTACATCAGGGAAGGAAATTGAATACCAAGATGCTATTGTGGAAGCTGCATGGCC  
TCTAGGCAATGCTGTAGAAGCCATATCAGCTTTACCTAAATTTGAGCGATTGATGT  
ATTTTGT

Figure 2.1.2 C

### Truncated-DM-PsNTP9 CDS

```
GAAATTTCTCTTACGCTGTAGTATTTCGATGCTGGTAGCACCGGTAGTCGCATTCA
TGTTTACCATTTTAAACCAGAACCCTAGATCTTCTTCATATTGGCAAAGGTGTTGAGT
ATTATAATAAGATAACACCTGGTTTGGAGTTCATACGCTAATAATCCAGAACAGGCT
GCAAATCTCTCATTCCACTTTTAGAGCAAGCAGAAGATGTCGTCCCCGACGATCT
TCAACCCAAGACACCCGTTAGACTTGGGGCAACTGCCGGTTTAAGGCTTTTGAATG
GAGATGCTTCTGAAAAGATATTGCAATCGGTAAGGGATAT
GCTGAGCAACAGAAGTACCTTCAACGTTCAACCAGACGCAGTTTCTATAATTGATG
GAACCCAAGAAGGTTCTTATCTATGGGTGACAGTTAACTATGCATTGGGAAATTTA
GGGAAAAAGTACACAAAAACAGTTGGAGTAATAGATCTTGGAGGTGGATCAGTTCA
AATGGCGTATGCAGTATTTAAAGAAAAGTCTAAAAATGCTCGAAAAGTTGCAGATG
GAGATGATCCATACATCAAGAAGGTTGTAAGGGAATACCATATGATCTCTAT
GTTACAGTTACTTACACTTCGGTAGAGAAGCATCTCGAG
CAGAGATTTTGAAGCTCACTCCTCGTTCTCCTAACCCCTTGCCTTTTAGCTGGATTT
AATGGAATCTATACATATTCAGGAGAAGAGTTTAAAGGCAACTGCTTACACTTCTGG
TGCAAACCTTTAATAAATGCAAAAACACAATTCGTAAGGCTCTTAAGTTGAACTATC
CTTGTCATATCAGAATTGCACTTTTGGTGGAAATTTGGAATGGTGGAGGAGGAAAT
GGACAGAAAAACCTTTTGGCTTCTTCATCTTTCTTTTACCTACCTGAAGATACCGG
TATGGTTGATGCAAGCACACCTAATTTCATACTTCGGCCG
GTCGATATTGAGACTAAAGCTAAAGAAGCTTGCAGCTTAAACTTCGAGGATGCGAA
ATCTACTTATCCATTTCTTGATAAGAAAAATGTAGCTTCATATGTATGCATGGATC
TTATATATCAGTATGTGTTACTCGTTGATGGATTTGGTCTTGATCCATTGCAAAAG
ATTACATCAGGGAAGGAAATTGAATACCAAGATGCTATTGTGGAAGCTGCATGGCC
TCTAGGCAATGCTGTAGAAGCCATATCAGCTTTACCTAAATTTGAGCGATTGATGT
ATTTTGT
```

**Figure 2.1.2** PsNTP9 and PsNTP9-DM protein-coding sequences are shown before and after modification for preparation of insertion to the pET22B plasmid. **A.** The PsNTP9 full length CDS was the template for both constructs. **B.** Shows the truncated version of the protein, where only deletions were used to prepare the coding sequence for insertion. **C.** The double mutant has two single nucleotide changes to create a second calmodulin binding domain.

Figure 2.1.3 A

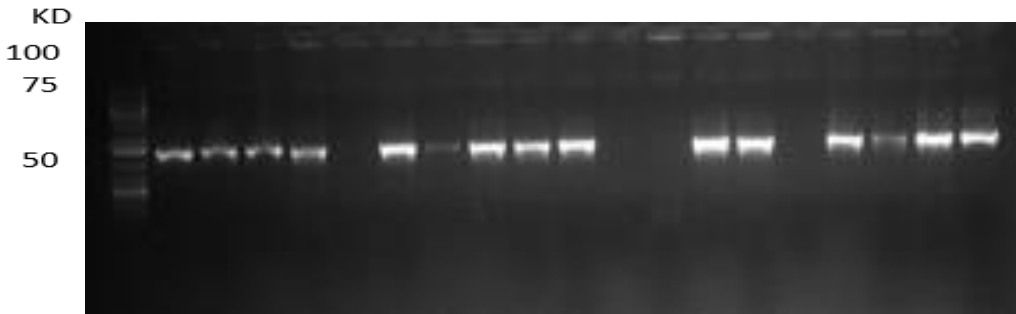


Figure 2.1.3 B

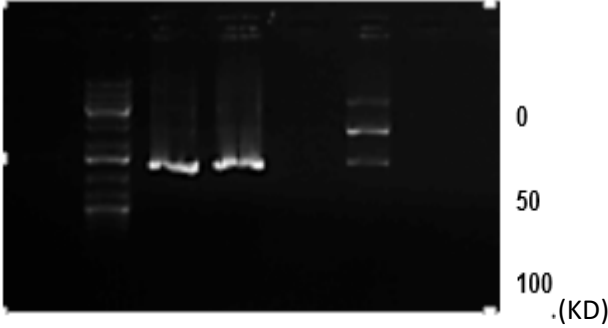


Figure 2.1.3 C

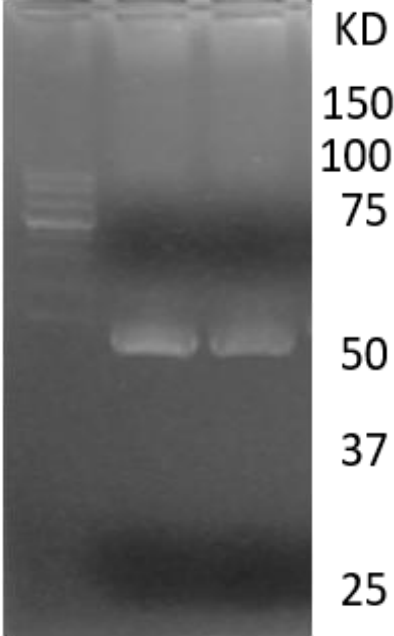


Figure 2.1.3 D

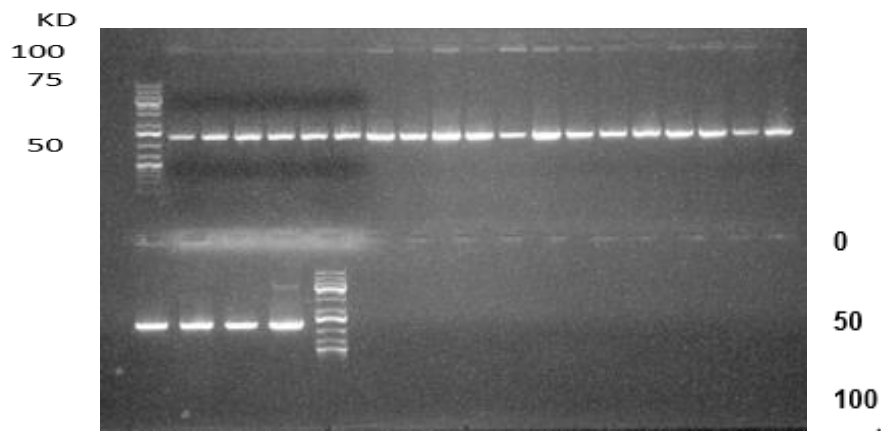


Figure 2.1.3 A. PCR product of Ps-NTP9–pET22B B. PCR product of PsNTP9-DM, C. Colony PCR of PsNTP9-pET22B, D. Colony PCR of PsNTP9-DM – pET22B.

**MUTATION 1: TCA → TTA (Ser to Leu)**

**MUTATION 2: CCA → CGA (Pro to Arg)**

**DOUBLE MUTATION : TCA → TTA (Ser to Leu)**  
**CCA → CGA (Pro to Arg)**

**Primers for cloning and colony PCR**

**NTP9-F40-NcoI**  
**ATGGCCATGGGAGAAATTCCTCTTAC**

**NTP9-R-BamHI**  
**TAAGGGATCCGAAACAAAATACATCAATC**

2.1.4 Mutations 1&2 shown at top were made by site directed mutagenesis to PsNTP9 in order to code for a second calmodulin binding domain for the PsNTP9-double mutant. The primers shown above were used for cloning and also colony PCR. The names above the sequences show the nuclease cut sites for insertion.

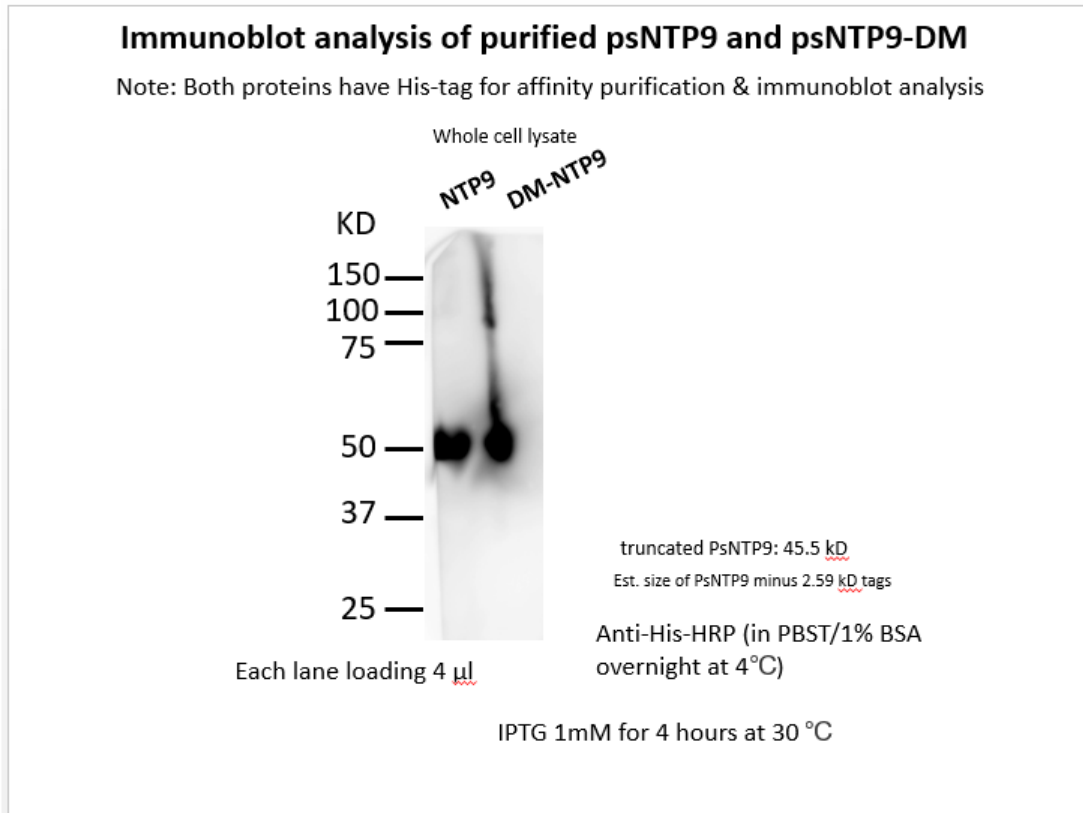


**Figure 2.2** The C-terminal His•Tag® sequence on PsNTP9 and PsNTP9-DM were detected by immunoblot using a horse radish peroxidase (HRP) conjugated antibody called HisProbe™ (Thermo-Scientific #15165)1:3500.

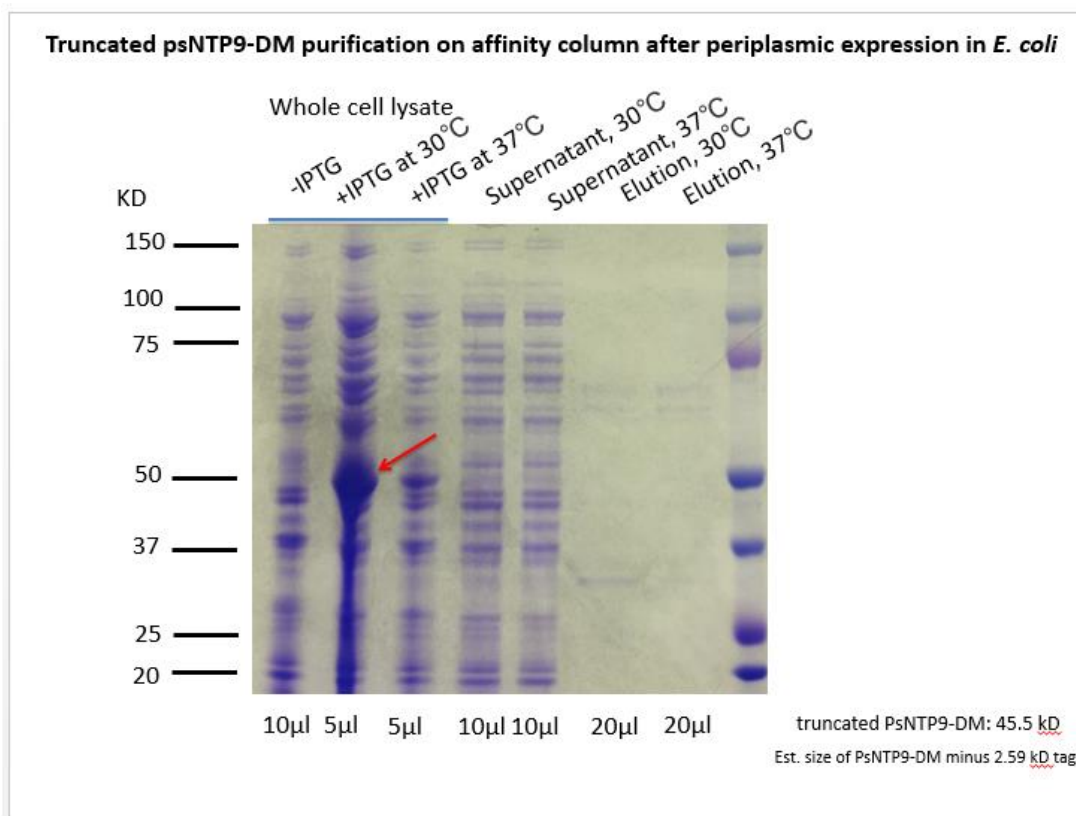


**Figure 3.1.1** The whole cell lysate, after induction by IPTG at 30°C shows the greatest induction, as determined by the darker band within the smear of proteins found in the raw protein extract that is indicated with the red arrow.

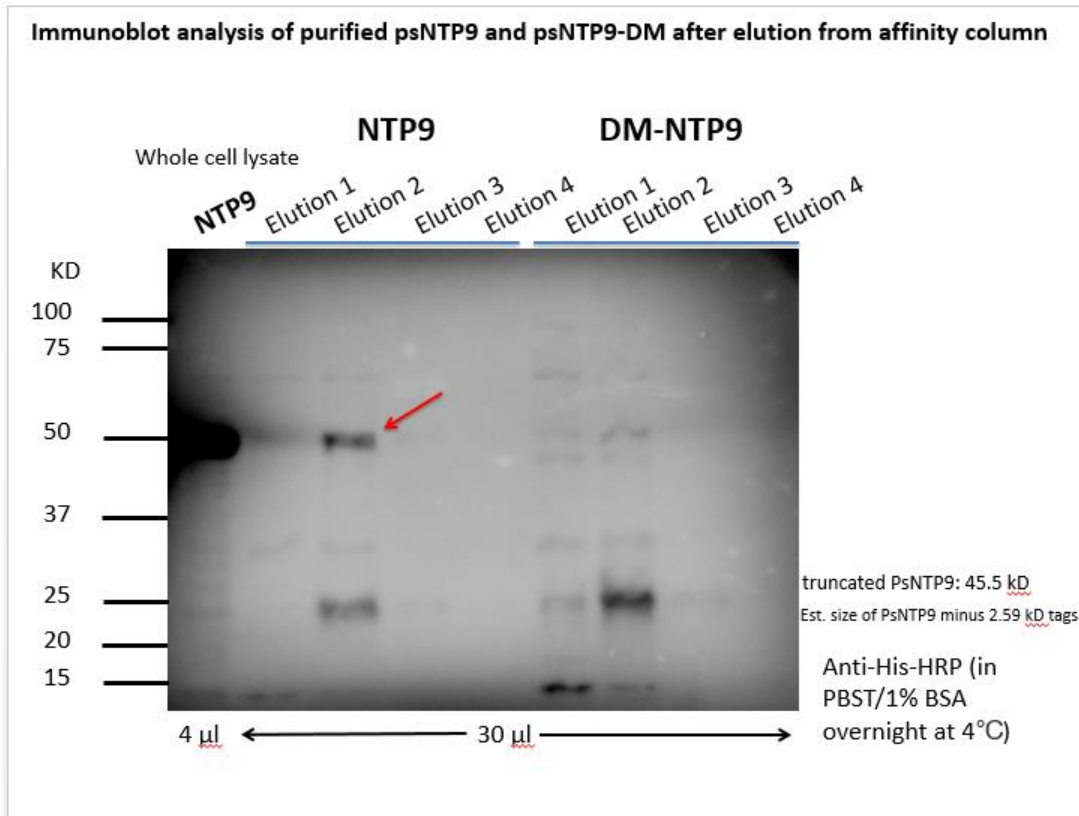


**Figure 3.2.1** Western blot showing truncated PsNTP9 and PsNTP9-DM concentrations in whole cell lysate and elution fractions after purification on affinity column. The red arrow points to a strong band in PsNTP9 elution 2 fraction. This band indicates a strong presence of PsNTP9, identified by antibody conjugation.



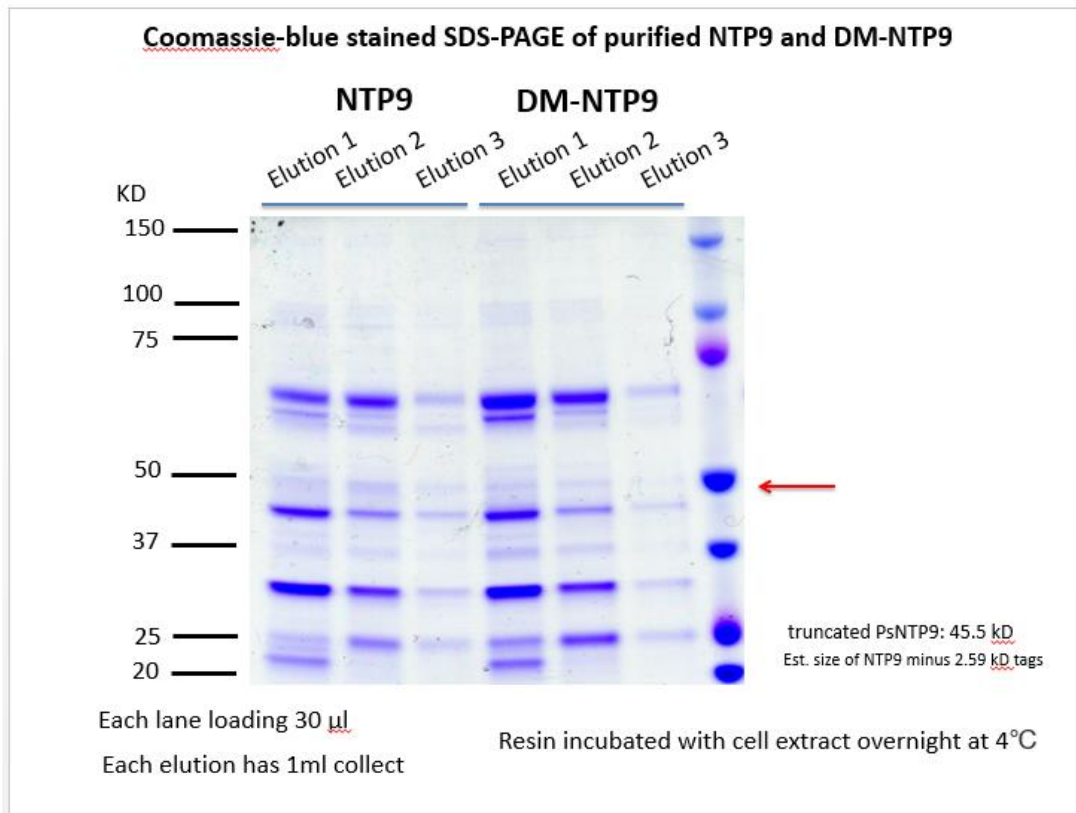


**Figure 3.2.2** This gel shows signal in each of the elution fractions 1 through 3, with the strongest bands in the first and second elution fractions. Elution 2 indicates the most protein at 50kD in both constructs.

FIGURE 4.2 A

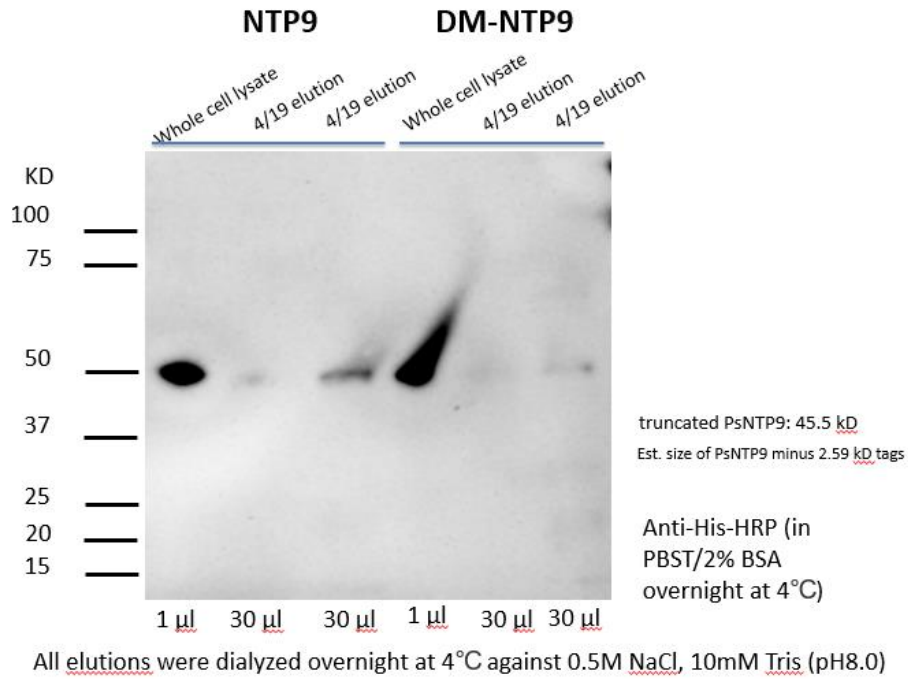
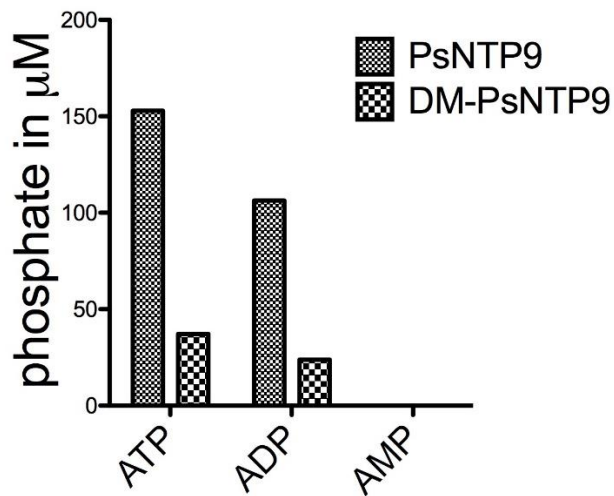


Figure 4.2 B



PsNTP9 and PsNTP9-DM apyrase assay used 03/28 elution protein. 50 μl of elution protein was used for each reaction. The concentration of PsNTP9 and PsNTP9-DM protein is 20.3 ng/μL and 22.1 ng/μL, respectively.

## Chapter 6: Discussion

There have been so many advances in genetic engineering that we now have multiple methods and resources for producing bioactive recombinant proteins, even human enzymes for use in medical treatment (Schmidt et al. 1999; Sockolosky et al., 2013). The pET22b plasmid is a member of the pET expression system commercially available from Novagen. pET22b has all the necessary selectivity, cloning, and other user-friendly features, including a histidine tag allowing for affinity column purification, and also an inducible periplasmic expression system using the *Lac* operon. Using this plasmid, it was possible to have a complete workable protocol for the production of testable quantities of PsNTP9 and PsNTP9-DM, a double mutant (DM) designed with a second calmodulin-binding domain.

PsNTP9 is a nuclear pea apyrase, which we have induced in *E. coli* with a periplasmic localization signal present in the pET22b vector. The addition of Isopropyl  $\beta$ -D-1-thiogalactopyranoside (IPTG), which is a molecular mimic of allolactose, stimulates the *Lac* operon by removing the Lac repressor. The hybrid T7 *lac* promoter and *lac I* gene encoding the repressor are included in the pET22b plasmid. Successful cloning was all that was required to have expression of our proteins of interest.

The DH5 $\alpha$  strain was developed by biologist Douglas Hanahan as a cloning strain with multiple mutations to enable high-efficiency transformations with a color change indicator for verification. Interestingly, this strain has been used for biological data storage experiments, presumably for its integrity. We used it to transform the

BL21 cells that were used for expression of PsNTP9 and PsNTP9-DM, for which it worked very well.

The expression of our proteins in the periplasm was important, and was done in order to try to avoid the formation of inclusion bodies, which is necessary to overcome in cytoplasmic overexpression (Sokolosky et al., 2013). When these insoluble aggregates form, steps must be taken to separate them. The aggregated proteins need to be treated with a denaturant or a detergent and refolded, which adds extra steps replete with complications, and could compromise the results of activity assays. By having our proteins expressed in the periplasm, isolation could be performed in native conditions. However, there is a potential complication: Protein expression could be so high that aggregates form even in the periplasm. If this does occur, it should be to a much lesser degree than happens in cytoplasmic expression, and is arguably unavoidable without changing the native conditions for extraction.

As described in Chapter 3, IMAC resin was used to select for the histidine tags added to the N-terminal of our PsNTP9 and PsNTP9-DM. IMAC stands for immobilized metal anion chromatography. Ni<sup>2+</sup> was the metal anion selected for its demonstrated ability to bind the 6xHis tag. There were some problems to overcome with this scheme, such as the natural occurrence of other proteins with domains rich in histidine residues. The specificity of the resin for the histidine ions needs to be high enough to bind our proteins of interest, but low enough to prevent excess binding of other proteins. When the specificity of the resin is too high, the resin quickly becomes saturated, and some amount of our tagged proteins washes through the affinity column. Imidazole is used in the incubation and elution of the affinity column. Raising

the amount of imidazole of the wash buffer used can reduce specificity, and potentially reduce non-specific binding.

Sometimes the specificity of Ni<sup>2+</sup> resin is high enough that a 6xHis tag may require additional measures to properly elute the proteins of interest. In other words, much of our protein may have been left on the resin. There are many measures that can be taken to increase the effectiveness of elution, though some solutions present their own problems or require special equipment. We kept 4 elution volumes and checked them separately, though it is sometimes recommended that serial dilutions be performed up to 20 times, and evaluate each fraction for protein concentration and size in kilodaltons (kD). As mentioned, increasing the concentration of imidazole affects the specificity of the resin. Raising the amount of imidazole in the elution buffer would likely elute more protein. This could be done in standard amounts on a gradient to find the right amount to elute as much protein as possible. Time wise this is exhausting, especially without using HPLC to segregate for our protein size. Changing the pH of the elution buffer could have the effect of increasing the volume of eluted protein, though it could also denature the proteins. Adding EDTA to the elution buffer in high enough concentration would undoubtedly remove everything from the resin, though this method would greatly reduce the concentration of our proteins of interest in the eluate. There are more options for increasing elution, but these were the ones we considered.

The purpose of this research, individually, is to characterize PsNTP9, a pea apyrase. However, an important impact of research in the field of extracellular ATP signaling is that the information discovered can be applied across kingdoms of organisms. Research conducted on plants may impact our understanding of human physiology, and vice versa. For instance, in the last 3 decades, NTPDases have been cloned and characterized in mammals, invertebrate animals, microbes and plants. Last year New Zealand scientists revealed the first structures of NTPDases from legume plant species *Trifolium repens* (7WC) and *Vigna unguiculata* subsp. *cylindrica* (DbLNP) (Summers et al, 2017). Study of the structure revealed that the apyrases have a central hinge region, and have at least two conformations depending on the molecule and co-factors bound. This phenomenon has been previously described in the brown rat, *Rattus norvegicus* and the bacteria *Legionella pneumophila*, and *Toxoplasma gondii* suggesting a common catalytic mechanism across the domains of life (Summers et al, 2017).

The field of NTP signaling has been expanded most in animal systems, due to the relevance to human health. The study of the impact of eATP, for example, on mammalian physiology covers a variety of systems and patho-physiological processes including vascular and nervous systems. Robson et al. (2006) describes acute effects on cellular metabolism, adhesion, activation and migration, as well as protracted impacts upon developmental responses, inclusive of cellular proliferation, differentiation and apoptosis, as seen with atherosclerosis, degenerative neurological diseases and rejection of transplanted organs and cells by the immune system. Future impacts may involve the development of new therapeutic strategies for organ

transplantation and cardiovascular, gastrointestinal and neurological diseases (Robson et al, 2006).

A number of different physiological effects of apyrase signaling in plants are known as well, including the operation of stomates. The opening and closing of stomates is concurrent with a release of ATP from the guard cells. This led to the discovery that eATP is involved with the opening and closing of stomates through the activation of a heterotrimeric G-protein phosphatase. This is confirmed by multiple studies (Hao et al., 2012; Clark et al., 2013). In *Arabidopsis thaliana* (At), AtAPY1, and AtAPY2 are known to be affected by changes in eATP. The discovery of this led to our understanding that AtAPY1&2 are upregulated upon wounding, cell expansion and hypertonic stress (Wu et al., 2007; Kim et al., 2009). Given these physiological effects, AtAPY1&2 were grouped with ecto-apyrases. Since 2012, there have been several more localization studies, with several asserting that expression is in the Golgi apparatus (Schiller et al., 2012; Chiu et al., 2012; Massalki et al., 2014). Given that the endomembrane system is involved with exocytosis, apyrase receptors located here could still be integral to signal transduction. As new components of nucleotide signaling are sought out, the search for homogeneity, or domain similarity has been a leading factor in their discovery and characterization.

## Chapter 7: Conclusions

*Pisum sativum* PsNTP9 was able to be truncated and modified, and two vectors were made by inserting PsNTP9 and the altered double mutant (PsNTP9-DM) into the pET22B plasmid. This success allowed for the cloning and transformation of *Escherichia coli* cells, which in turn allowed us to express PsNTP9 and PsNTP9-DM ectopically. The transformed bacteria were able to be grown and have expression induced. Upon fractionation and purification, a significant yield a significant amount of protein usable for characterization was obtained. It would have been desirable to have some calmodulin to use in conjunction with NTP9, and DM especially, in the apyrase activity assay. I believe that there could be a significant increase in activity in both constructs, and perhaps more-so with calmodulin bound DM. Additionally, antibodies are being developed for PsNTP9, and these will be directly useful in this research, allowing for more accurate identification.

The purification protocol used still requires optimization, and though it was used to some success, it can still be improved. Perhaps the use of a histidine tag can be done away with once the antibodies being tested are proven viable. Another type of affinity chromatography, perhaps cross-linking antibodies with sephadex, may be used to isolate proteins using the antibodies being developed. The use of such a tool would be invaluable to the current research, as it would enable the exclusion of the multitude of histidine containing proteins that are co-purified and co-identified using histidine's affinity for metal ions. Perhaps the antibodies might be used to identify other potential purinoceptors as well.



There are a few measures which might still be taken to optimize expression, fractionation, and purification, even without new antibodies. Perhaps using a larger cell culture to express and isolate from, or a slightly lower quantity of IPTG would reduce aggregation, allowing more protein of interest to bind to the affinity column.

The results of the apyrase assay were not exactly as expected; PsNTP9 had more activity than PsNTP9-DM on the apyrase and phosphate assays performed. This could be due to having nearly equal concentrations of protein, but lower concentrations of the proteins of interest. A Western blot using a more specific antibody could give an accurate determination of this. Possible unequal amounts of our proteins of interest could be a source of complication with the activity assays.

Though there are still a few improvements to be made with these methods, the results have shown that they can be effective in advancing this field of study. Researchers must continue to look across the Kingdoms for clues, and use proven techniques as well as experimentation in order to resolve them.

## References

- Burnstock, G.** (2007). Purine and pyrimidine receptors. *Cellular and Molecular Life Sciences*, 64(12), 1471.
- Burnstock, G.** (1972). Purinergic nerves. *Pharmacological reviews*, 24(3), 509-581.
- Cho, S. H., Choi, J., & Stacey, G.** (2017). Molecular mechanism of plant recognition of extracellular ATP. *Advances in Experimental Medical Biology* 1051:233-253.
- Choi, J., Tanaka, K., Cao, Y., Qi, Y., Qiu, J., Liang, Y., ... & Stacey, G.** (2014). Identification of a plant receptor for extracellular ATP. *Science*, 343(6168), 290-294.
- Clark, G., & Roux, S. J.** (2011). Apyrases, extracellular ATP and the regulation of growth. *Current Opinion in Plant Biology*, 14(6), 700-706.
- Clark, G., Fraley, D., Steinebrunner, I., Cervantes, A., Onyirimba, J., Liu, A., ... & Roux, S. J.** (2011). Extracellular nucleotides and apyrases regulate stomatal aperture in Arabidopsis. *Plant Physiology*, 156(4), 1740-1753.
- Clark, G. B., Morgan, R. O., Fernandez, M. P., Salmi, M. L., & Roux, S. J.** (2014). Breakthroughs spotlighting roles for extracellular nucleotides and apyrases in stress responses and growth and development. *Plant Science*, 225, 107-116.
- Demidchik, V., Shang, Z., Shin, R., Thompson, E., Rubio, L., Laohavisit, A., ... & Schachtman, D. P.** (2009). Plant extracellular ATP signalling by plasma membrane NADPH oxidase and Ca<sup>2+</sup> channels. *The Plant Journal*, 58(6), 903-913.

**Demidchik, V., Shang, Z., Shin, R., Colaço, R., Laohavisit, A., Shabala, S., & Davies, J. M.** (2011). Receptor-like activity evoked by extracellular ADP in Arabidopsis root epidermal plasma membrane. *Plant Physiology*, 156(3), 1375-1385.

**Fountain, S. J., Cao, L., Young, M. T., & North, R. A.** (2008). Permeation properties of a P2X receptor in the green algae *Ostreococcus tauri*. *Journal of Biological Chemistry*, 283(22), 15122-15126.

**Hao, L. H., Wang, W. X., Chen, C., Wang, Y. F., Liu, T., Li, X., & Shang, Z. L.** (2012). Extracellular ATP promotes stomatal opening of *Arabidopsis thaliana* through heterotrimeric G protein  $\alpha$  subunit and reactive oxygen species. *Molecular Plant*, 5(4), 852-864.

**Jeter, C. R., Tang, W., Henaff, E., Butterfield, T., & Roux, S. J.** (2004). Evidence of a novel cell signaling role for extracellular adenosine triphosphates and diphosphates in *Arabidopsis*. *The Plant Cell*, 16(10), 2652-2664.

**Lim, M. H., Wu, J., Yao, J., Gallardo, I. F., Dugger, J. W., Webb, L. J., ... & Roux, S. J.** (2014). Apyrase suppression raises extracellular ATP levels and induces gene expression and cell wall changes characteristic of stress responses. *Plant Physiology*, 164(4), 2054-2067.

**Liu, X., Wu, J., Clark, G., Lundy, S., Lim, M., Arnold, D., ... & Roux, S. J.** (2012). Role for apyrases in polar auxin transport in *Arabidopsis*. *Plant Physiology*, 160(4), 1985-1995.

**Robson, S. C., Sévigny, J., & Zimmermann, H.** (2006). The E-NTPDase family of ectonucleotidases: structure function relationships and pathophysiological significance. *Purinergic Signalling*, 2(2), 409.

**Roux, S. J., & Steinebrunner, I.** (2007). Extracellular ATP: an unexpected role as a signaler in plants. *Trends in Plant Science*, 12(11), 522-527.

**Roux, S. J. (2014).** A start point for extracellular nucleotide signaling. *Molecular Plant*, 7(6), 937-938.

**Sokolosky, J. T., & Szoka, F. C.** (2013). Periplasmic production via the pET expression system of soluble, bioactive human growth hormone. *Protein Expression and Purification*, 87(2), 129-135.

**Song, C. J., Steinebrunner, I., Wang, X., Stout, S. C., & Roux, S. J.** (2006). Extracellular ATP induces the accumulation of superoxide via NADPH oxidases in Arabidopsis. *Plant Physiology*, 140(4), 1222-1232.

**Schmidt, M., Babu, K., Khanna, N., Marten, S., & Rinas, U.** (1999). Temperature-induced production of recombinant human insulin in high-cell density cultures of recombinant Escherichia coli. *Journal of Biotechnology*, 68(1), 71-83.

**Summers, E. L., Cumming, M. H., Oulavallickal, T., Roberts, N., & Arcus, V. L.** (2017). Structures and kinetics for plant nucleoside triphosphate diphosphohydrolases (NTPDases) support a domain motion catalytic mechanism. *Protein Science*. 26(8):1627-1638.

**Tanaka, K., Choi, J., Cao, Y., & Stacey, G.** (2014). Extracellular ATP acts as a damage-associated molecular pattern (DAMP) signal in plants. *Frontiers in plant Science*, 5, 446.

**Tanaka, K., Gilroy, S., Jones, A. M., & Stacey, G.** (2010). Extracellular ATP signaling in plants. *Trends in Cell Biology*, 20(10), 601-608.

**Tang, W., Brady, S. R., Sun, Y., Muday, G. K., & Roux, S. J.** (2003). Extracellular ATP inhibits root gravitropism at concentrations that inhibit polar auxin transport. *Plant Physiology*, 131(1), 147-154.

**Tripathi, D., & Tanaka, K.** (2018). A crosstalk between extracellular ATP and jasmonate signaling pathways for plant defense. *Plant Signaling & Behavior*, 176, 1-13.

## Vita

Michael Andrew Wallen Jr. was born in San Antonio, TX. He graduated from John Marshall HS there in 1997, and enrolled at UTSA in the following year, studying primarily in biology. In 1998, he joined the US Navy and served 6 years as a nuclear qualified machinist mate on the Harry S. Truman aircraft carrier. Upon returning home to San Antonio in 2004, Michael found work at the UTSA facilities department and completed a bachelor's degree in Applied Science and Technology in 2009. In 2010 he moved to Austin, but continued to study at UTSA for 2 years to meet the requirements to attend grad school at UT in Austin in the College of Natural Sciences. Michael accepted a Plant Biology fellowship and worked as a TA while earning his master's degree.

Permanent Address:

11308 Brenham St

Manor, TX, 78653

Thesis typed by author.